Multidimensional replica-exchange method for free-energy calculations

Yuji Sugita, Akio Kitao, and Yuko Okamoto

Citation: J. Chem. Phys. **113**, 6042 (2000); doi: 10.1063/1.1308516
View online: https://doi.org/10.1063/1.1308516
View Table of Contents: http://aip.scitation.org/toc/jcp/113/15
Published by the American Institute of Physics

Multidimensional replica-exchange method for free-energy calculations

Yuji Sugita[a)]
Department of Theoretical Studies, Institute for Molecular Science, Okazaki, Aichi 444-8585, Japan

Akio Kitao[b)]
Department of Chemistry, Graduate School of Science, Kyoto University, Kyoto 606-8502, Japan

Yuko Okamoto[c)]
Department of Theoretical Studies, Institute for Molecular Science, Okazaki, Aichi 444-8585, Japan, and Department of Functional Molecular Science, The Graduate University for Advanced Studies, Okazaki, Aichi 444-8585, Japan

(Received 26 May 2000; accepted 19 July 2000)

We have developed a new simulation algorithm for free-energy calculations. The method is a multidimensional extension of the replica-exchange method. While pairs of replicas with different temperatures are exchanged during the simulation in the original replica-exchange method, pairs of replicas with different temperatures and/or different parameters of the potential energy are exchanged in the new algorithm. This greatly enhances the sampling of the conformational space and allows accurate calculations of free energy in a wide temperature range from a single simulation run, using the weighted histogram analysis method. © *2000 American Institute of Physics.* [S0021-9606(00)50739-9]

I. INTRODUCTION

In complex systems such as a system of proteins, it is difficult to obtain accurate canonical distributions at low temperatures by the conventional molecular dynamics (MD) or Monte Carlo (MC) simulations. This is because there exist a huge number of local-minimum states in the potential energy surface, and the simulations tend to get trapped in one of the local-minimum states. One popular way to overcome this difficulty is to perform a *generalized-ensemble* simulation, which is based on non-Boltzmann probability weight factors so that a random walk in energy space may be realized (for a review see Ref. 1). The random walk allows the simulation to go over any energy barrier and sample much wider configurational space than by conventional methods. Monitoring the energy in a single simulation run, one can obtain not only the global-minimum-energy state but also any thermodynamic quantities as a function of temperature for a wide temperature range. The latter is made possible by the single-histogram[2] or multiple-histogram[3] reweighting techniques (an extension of the multiple-histogram method is also referred to as the weighted histogram analysis method (WHAM)[4]).

Three of the most well-known generalized-ensemble methods are perhaps *multicanonical algorithm*,[5] *simulated tempering*,[6,7] and *replica-exchange method*.[8–12] (The replica-exchange method is also referred to as *replica Monte Carlo method*[9], *multiple Markov chain method*,[11] and *parallel tempering*.[12]) These algorithms have already been used in many applications in protein and related systems (see, for instance, Refs. 13–36 for multicanonical algorithm, Refs. 37–40 for simulated tempering, and Refs. 41–45 for replica-exchange method).

The replica-exchange method (REM) has been drawing much attention recently because the probability weight factors are essentially known *a priori*, whereas they are not in most other generalized-ensemble algorithms (and have to be determined by a tedious procedure). In REM the generalized ensemble consists of noninteracting copies (or replicas) of the original system with different temperatures. During a parallel MD or MC simulation of each replica, a pair of replicas are exchanged every few steps. This procedure enforces random walks in the replica (temperature) space.

In a previous work[44] we worked out the details for the replica-exchange molecular dynamics algorithm. In this article we present a multidimensional extension of the replica-exchange method (similar generalizations of REM can also be found in Refs. 46 and 47). In the new algorithm, pairs of replicas with different temperatures and/or different parameters of the potential energy are exchanged. As an example of the applications of the multidimensional replica-exchange method, we discuss free-energy calculations in detail.

The umbrella sampling method[48] and free-energy perturbation method, which is a special case of umbrella sampling, have been widely used to calculate the free energies in chemical processes.[48–57] In the umbrella sampling method, a reaction coordinate is chosen and free-energy profiles along the reaction coordinate are calculated. A series of independent simulations are performed to sample the relevant range of the coordinate. To cover the entire range of the coordinate, biasing potentials, which are called ''umbrella potentials,'' are imposed. Thus, the system is restrained to remain near the prechosen value of the reaction coordinate specified by each umbrella potential, and a series of simulations with different umbrella potentials are performed. WHAM[4] is often

a)Electronic mail: sugita@ims.ac.jp
b)Electronic mail: kitao@qchem.kuchem.kyoto-u.ac.jp
c)Electronic mail: okamotoy@ims.ac.jp

employed to calculate the free-energy profiles from the histograms obtained by each simulation.

Although the effectiveness of the umbrella sampling method is well known, its successful implementation requires a careful fine tuning. For instance, the choice of the umbrella potentials is very important. If the potentials are too strong, the conformational space sampled by each simulation becomes quite narrow. If the potentials are too weak, on the other hand, the system does not remain near the prechosen value of the reaction coordinate. The values of the coupling parameters λ for the umbrella potentials should also be carefully chosen. Various generalizations of the umbrella sampling method have thus been introduced to sample the potential energy surface more effectively. The λ-*dynamics*[58–60] is such an example, where the coupling parameter λ is treated as a dynamical variable. Another example is the *multicanonical WHAM,*[35] which combines the umbrella sampling with the multicanonical algorithm. In the present article we develop yet another generalization of the umbrella sampling method (we refer to this method as *replica-exchange umbrella sampling*), which is based on the multidimensional extension of the replica-exchange method.

In Sec. II the multidimensional extension of the replica-exchange method is described in detail. In particular, the replica-exchange umbrella sampling method is introduced. In Sec. III the results of the application of replica-exchange umbrella sampling to a blocked alanine trimer are given. Section IV is devoted to conclusions.

II. METHODS

Before we describe the *multidimensional replica-exchange method* (MREM), let us briefly review the original *replica-exchange method* (REM)[8–12] (see Ref. 44 for details).

We consider a system of N atoms with their coordinate vectors and momentum vectors denoted by $q \equiv \{\mathbf{q}_1,\ldots,\mathbf{q}_N\}$ and $p \equiv \{\mathbf{p}_1,\ldots,\mathbf{p}_N\}$, respectively. The Hamiltonian $H(q,p)$ of the system is the sum of the kinetic energy $K(p)$ and the potential energy $E(q)$,

$$H(q,p) = K(p) + E(q). \tag{1}$$

In the canonical ensemble at temperature T, each state $x \equiv (q,p)$ with the Hamiltonian $H(q,p)$ is weighted by the Boltzmann factor,

$$W_B(x) = e^{-\beta H(q,p)}, \tag{2}$$

where the inverse temperature β is defined by $\beta = 1/k_B T$ (k_B is Boltzmann's constant).

The generalized ensemble for REM consists of M *noninteracting* copies (or, replicas) of the original system in the canonical ensemble at M different temperatures T_m ($m = 1,\ldots,M$). We arrange the replicas so that there is always exactly one replica at each temperature. Then there is a one-to-one correspondence between replicas and temperatures; the label i ($i = 1,\ldots,M$) for replicas is a permutation of the label m ($m = 1,\ldots,M$) for temperatures, and vice versa,

$$\begin{cases} i = i(m) \equiv f(m), \\ m = m(i) \equiv f^{-1}(i), \end{cases} \tag{3}$$

where $f(m)$ is a permutation function of m and $f^{-1}(i)$ is its inverse.

Let $X = \{x_1^{[i(1)]},\ldots,x_M^{[i(M)]}\} = \{x_{m(1)}^{[1]},\ldots,x_{m(M)}^{[M]}\}$ stand for a ''state'' in this generalized ensemble. Here, the superscript and the subscript in $x_m^{[i]}$ label the replica and the temperature, respectively. The state X is specified by the M sets of coordinates $q^{[i]}$ and momenta $p^{[i]}$ of N atoms in replica i at temperature T_m,

$$x_m^{[i]} \equiv (q^{[i]}, p^{[i]})_m. \tag{4}$$

Because the replicas are noninteracting, the weight factor for the state X in this generalized ensemble is given by the product of Boltzmann factors for each replica (or at each temperature),

$$\begin{aligned} W_{\mathrm{REM}}(X) &= \exp\left\{ -\sum_{i=1}^{M} \beta_{m(i)} H(q^{[i]}, p^{[i]}) \right\} \\ &= \exp\left\{ -\sum_{m=1}^{M} \beta_m H(q^{[i(m)]}, p^{[i(m)]}) \right\}, \end{aligned} \tag{5}$$

where $i(m)$ and $m(i)$ are the permutation functions in Eq. (3).

We now consider exchanging a pair of replicas in the generalized ensemble. Suppose we exchange replicas i and j which are at temperatures T_m and T_n, respectively,

$$X = \{\ldots, x_m^{[i]}, \ldots, x_n^{[j]}, \ldots\} \rightarrow X' = \{\ldots, x_m^{[j]\prime}, \ldots, x_n^{[i]\prime}, \ldots\}. \tag{6}$$

The exchange of replicas can be written in more detail as

$$\begin{cases} x_m^{[i]} \equiv (q^{[i]}, p^{[i]})_m & \rightarrow x_m^{[j]\prime} \equiv (q^{[j]}, p^{[j]\prime})_m, \\ x_n^{[j]} \equiv (q^{[j]}, p^{[j]})_n & \rightarrow x_n^{[i]\prime} \equiv (q^{[i]}, p^{[i]\prime})_n, \end{cases} \tag{7}$$

where the momenta are uniformly rescaled according to[44]

$$\begin{cases} p^{[i]\prime} & \equiv \sqrt{\dfrac{T_n}{T_m}}\, p^{[i]}, \\ p^{[j]\prime} & \equiv \sqrt{\dfrac{T_m}{T_n}}\, p^{[j]}. \end{cases} \tag{8}$$

In order for this exchange process to converge toward the equilibrium distribution based on Eq. (5), it is sufficient to impose the detailed balance condition on the transition probability $w(X \rightarrow X')$,

$$W_{\mathrm{REM}}(X)\, w(X \rightarrow X') = W_{\mathrm{REM}}(X')\, w(X' \rightarrow X). \tag{9}$$

From Eqs. (1), (5), (8), and (9), we have

$$\frac{w(X \rightarrow X')}{w(X' \rightarrow X)} = \exp(-\Delta), \tag{10}$$

where

$$\Delta = \beta_m (E(q^{[j]}) - E(q^{[i]})) - \beta_n (E(q^{[j]}) - E(q^{[i]})), \tag{11}$$

$$= (\beta_m - \beta_n)(E(q^{[j]}) - E(q^{[i]})). \tag{12}$$

This can be satisfied, for instance, by the usual Metropolis criterion,[61]

$$w(X\rightarrow X')\equiv w(x_m^{[i]}|x_n^{[j]})=\begin{cases}1, & \text{for } \Delta\leqslant 0,\\ \exp(-\Delta), & \text{for } \Delta>0.\end{cases} \tag{13}$$

Note that because of the velocity rescaling of Eq. (8) the kinetic energy terms are cancelled out in Eqs. (11) [and (12)] and that the same criterion, Eqs. (12) and (13), which was originally derived for the Monte Carlo algorithm,[8–12] is recovered.[44]

A simulation of the *replica-exchange method* (REM)[8–12] is then realized by alternately performing the following two steps:

(1) Each replica in canonical ensemble of the fixed temperature is simulated *simultaneously* and *independently* for a certain MC or MD steps.
(2) A pair of replicas, say $x_m^{[i]}$ and $x_n^{[j]}$, are exchanged with the probability $w(x_m^{[i]}|x_n^{[j]})$ in Eq. (13).

In the present work, we employ the molecular dynamics algorithm for step 1. Note that in step 2 we exchange only pairs of replicas corresponding to neighboring temperatures, because the acceptance ratio of the exchange decreases exponentially with the difference of the two β's [see Eqs. (12) and (13)]. Note also that whenever a replica exchange is accepted in step 2, the permutation functions in Eq. (3) are updated.

The major advantage of REM over other generalized-ensemble methods such as multicanonical algorithm[5] and simulated tempering[6,7] lies in the fact that the weight factor is *a priori* known [see Eq. (5)], while in the latter algorithms the determination of the weight factors can be very tedious and time-consuming. A random walk in ''temperature space'' is realized for each replica, which in turn induces a random walk in potential energy space. This alleviates the problem of getting trapped in states of energy local minima.

We now present our multidimensional extension of REM, which we refer to as the *multidimensional replica-exchange method* (MREM). The crucial observation that led to the new algorithm is: As long as we have *M noninteracting* replicas of the original system, the Hamiltonian $H(q,p)$ of the system does not have to be identical among the replicas and it can depend on a parameter with different parameter values for different replicas. Namely, we can write the Hamiltonian for the i-th replica at temperature T_m as

$$H_m(q^{[i]},p^{[i]})=K(p^{[i]})+E_{\lambda_m}(q^{[i]}), \tag{14}$$

where the potential energy E_{λ_m} depends on a parameter λ_m and can be written as

$$E_{\lambda_m}(q^{[i]})=E_0(q^{[i]})+\lambda_m V(q^{[i]}). \tag{15}$$

This expression for the potential energy is often used in simulations. For instance, in umbrella sampling,[48] $E_0(q)$ and $V(q)$ can be respectively taken as the original potential energy and the ''biasing'' potential energy with the coupling parameter λ_m. In simulations of spin systems, on the other hand, $E_0(q)$ and $V(q)$ (here, q stands for spins) can be respectively considered as the zero-field term and the magnetization term coupled with the external field λ_m.

While replica i and temperature T_m are in one-to-one correspondence in the original REM, replica i and ''parameter set'' $\Lambda_m\equiv(T_m,\lambda_m)$ are in one-to-one correspondence in the new algorithm. Hence, the present algorithm can be considered as a multidimensional extension of the original replica-exchange method where the ''parameter space'' is one dimensional (i.e., $\Lambda_m=T_m$). Because the replicas are noninteracting, the weight factor for the state X in this new generalized ensemble is again given by the product of Boltzmann factors for each replica [see Eq. (5)],

$$\begin{aligned}W_{\mathrm{MREM}}(X)&=\exp\left\{-\sum_{i=1}^{M}\beta_{m(i)}H_{m(i)}(q^{[i]},p^{[i]})\right\}\\&=\exp\left\{-\sum_{m=1}^{M}\beta_m H_m(q^{[i(m)]},p^{[i(m)]})\right\},\end{aligned} \tag{16}$$

where $i(m)$ and $m(i)$ are the permutation functions in Eq. (3). Then the same derivation that led to the original replica-exchange criterion [Eq. (13)] follows, and we have the following transition probability of replica exchange [see Eq. (11)]:

$$w(X\rightarrow X')\equiv w(x_m^{[i]}|x_n^{[j]})=\begin{cases}1, & \text{for } \Delta\leqslant 0,\\ \exp(-\Delta), & \text{for } \Delta>0,\end{cases} \tag{17}$$

where

$$\Delta=\beta_m(E_{\lambda_m}(q^{[j]})-E_{\lambda_m}(q^{[i]}))-\beta_n(E_{\lambda_n}(q^{[j]})-E_{\lambda_n}(q^{[i]})). \tag{18}$$

Here, E_{λ_m} and E_{λ_n} are the total potential energies [see Eq. (15)]. Note that we need to newly evaluate the potential energy for exchanged coordinates, $E_{\lambda_m}(q^{[j]})$ and $E_{\lambda_n}(q^{[i]})$, because E_{λ_m} and E_{λ_n} are in general different functions. The method is particularly suitable for parallel computers. Because one can minimize the amount of information exchanged among nodes, it is best to assign each replica to each node (exchanging T_m, E_{λ_m} and T_n, E_{λ_n} among nodes is much faster than exchanging coordinates and momenta). This means that we keep track of the permutation function $m(i;t)=f^{-1}(i;t)$ in Eq. (3) as a function of MD step t throughout the simulation.

For obtaining the canonical distributions, the weighted histogram analysis method (WHAM)[4] is particularly suitable. Suppose we have made a single run of the present replica-exchange simulation with M replicas that correspond to M different parameter sets $\Lambda_m\equiv(T_m,\lambda_m)$ $(m=1,\ldots,M)$. Let $N_m(E_0,V)$ and n_m be, respectively, the potential-energy histogram and the total number of samples obtained for the m-th parameter set Λ_m. The expectation value of a physical quantity A for any potential-energy parameter value λ at any temperature $T=1/k_B\beta$ is then given by[3,4]

$$\langle A\rangle_{T,\lambda}=\frac{\sum_{E_0,V}A(E_0,V)P_{T,\lambda}(E_0,V)}{\sum_{E_0,V}P_{T,\lambda}(E_0,V)}, \tag{19}$$

where

$$P_{T,\lambda}(E_0,V)=\left[\frac{\sum_{m=1}^{M} g_m^{-1}N_m(E_0,V)}{\sum_{m=1}^{M} n_m g_m^{-1} e^{f_m-\beta_m E_{\lambda_m}}}\right] e^{-\beta E_\lambda}, \quad (20)$$

and

$$e^{-f_m}=\sum_{E_0,V} P_{T_m,\lambda_m}(E_0,V). \quad (21)$$

Here, $g_m=1+2\tau_m$, and τ_m is the integrated autocorrelation time at temperature T_m with the parameter value λ_m. Note that the unnormalized probability distribution $P_{T,\lambda}(E_0,V)$ and the ''dimensionless'' Helmholtz free energy f_m in Eqs. (20) and (21) are solved self-consistently by iteration.[3,4]

We can use this new replica-exchange method for free-energy calculations. We first describe the free-energy perturbation case. The potential energy is given by

$$E_\lambda(q)=E_I(q)+\lambda(E_F(q)-E_I(q)), \quad (22)$$

where E_I and E_F are the potential energy for a ''wild-type'' molecule and a ''mutated'' molecule, respectively. Note that this equation has the same form as Eq. (15).

Our replica-exchange simulation is performed for M replicas with M different values of the parameters $\Lambda_m=(T_m,\lambda_m)$. Since $E_{\lambda=0}(q)=E_I(q)$ and $E_{\lambda=1}(q)=E_F(q)$, we should choose enough λ_m values distributed in the range between 0 and 1 so that we may have sufficient replica exchanges. From the simulation, M histograms $N_m(E_I,E_F-E_I)$, or equivalently $N_m(E_I,E_F)$, are obtained. The Helmholtz free-energy difference of ''mutation'' at temperature T, $\Delta F\equiv F_{\lambda=1}-F_{\lambda=0}$, can then be calculated from

$$\exp(-\beta\Delta F)=\frac{Z_{T,\lambda=1}}{Z_{T,\lambda=0}}=\frac{\sum_{E_I,E_F} P_{T,\lambda=1}(E_I,E_F)}{\sum_{E_I,E_F} P_{T,\lambda=0}(E_I,E_F)}, \quad (23)$$

where $P_{T,\lambda}(E_I,E_F)$ are obtained from the WHAM equations of Eqs. (20) and (21).

We now describe another free-energy calculation based on MREM applied to umbrella sampling,[48] which we refer to as *replica-exchange umbrella sampling* (REUS). The potential energy is a generalization of Eq. (15) and is given by

$$E_{\boldsymbol{\lambda}}(q)=E_0(q)+\sum_{l=1}^{L}\lambda^{(l)}V_l(q), \quad (24)$$

where $E_0(q)$ is the original unbiased potential, $V_l(q)$ $(l=1,\ldots,L)$ are the biasing (umbrella) potentials, and $\lambda^{(l)}$ are the corresponding coupling constants $[\boldsymbol{\lambda}=(\lambda^{(1)},\ldots,\lambda^{(L)})]$. Introducing a ''reaction coordinate'' ξ, the umbrella potentials are usually written as harmonic restraints,

$$V_l(q)=k_l[\xi(q)-d_l]^2, \quad (l=1,\ldots,L), \quad (25)$$

where d_l are the midpoints and k_l are the strengths of the restraining potentials. We prepare M replicas with M different values of the parameters $\boldsymbol{\Lambda}_m=(T_m,\boldsymbol{\lambda}_m)$, and the replica-exchange simulation is performed. Since the umbrella potentials $V_l(q)$ in Eq. (25) are all functions of the reaction coordinate ξ only, we can take the histogram $N_m(E_0,\xi)$ instead of $N_m(E_0,V_1,\ldots,V_L)$. The WHAM equations of Eqs. (20) and (21) can then be written as

$$P_{T,\boldsymbol{\lambda}}(E_0,\xi)=\left[\frac{\sum_{m=1}^{M} g_m^{-1}N_m(E_0,\xi)}{\sum_{m=1}^{M} n_m g_m^{-1} e^{f_m-\beta_m E_{\boldsymbol{\lambda}_m}}}\right] e^{-\beta E_{\boldsymbol{\lambda}}}, \quad (26)$$

and

$$e^{-f_m}=\sum_{E_0,\xi} P_{T_m,\boldsymbol{\lambda}_m}(E_0,\xi). \quad (27)$$

The expectation value of a physical quantity A is now given by [see Eq. (19)]

$$\langle A\rangle_{T,\boldsymbol{\lambda}}=\frac{\sum_{E_0,\xi} A(E_0,\xi)P_{T,\boldsymbol{\lambda}}(E_0,\xi)}{\sum_{E_0,\xi} P_{T,\boldsymbol{\lambda}}(E_0,\xi)}. \quad (28)$$

The potential of mean force (PMF), or free energy as a function of the reaction coordinate, of the original, unbiased system at temperature T is given by

$$\mathcal{W}_{T,\boldsymbol{\lambda}=\{0\}}(\xi)=-k_BT\ln\left[\sum_{E_0} P_{T,\boldsymbol{\lambda}=\{0\}}(E_0,\xi)\right], \quad (29)$$

where $\{0\}=(0,\ldots,0)$. In the examples presented below, replicas were chosen so that the potential energy for each replica includes exactly one (or zero) biasing potential.

III. RESULTS AND DISCUSSION

One of the applications of MREM, *replica-exchange umbrella sampling* (REUS), was tested for the system of a blocked peptide, alanine trimer. The N and C termini of the peptide were blocked with acetyl and N-methyl groups, respectively. Since the thermodynamic behavior of this peptide was extensively studied by the conventional umbrella sampling,[51] it is a good test case to examine the effectiveness of the new method. All calculations were based on MD simulations, and the force field parameters were taken from the all-atom version of AMBER[62] with a distance-dependent dielectric, $\epsilon=r$, which mimics the presence of solvent. The computer code developed in Refs. 56 and 63, which is based on Version 2 of PRESTO,[64] was used. The temperature during the MD simulations was controlled by the constraint method.[65,66] The unit time step was set to 0.5 fs, and we made an MD simulation of 4×10^6 time steps (or 2.0 ns) for each replica, starting from an extended conformation. The data were stored every 20 steps (or 10 fs) for a total of 2×10^5 snapshots. (Before taking the data, we made regular canonical MD simulations of 100 ps for thermalization. For replica-exchange simulations an additional REM simulation of 100 ps was made for further thermalization.)

In Table I we summarize the parameters characterizing the replicas for the simulations performed in the present work. They are one original replica-exchange simulation (REM1), two replica-exchange umbrella sampling simula-

TABLE I. Summary of the replica parameters for the present simulations.

Run[a]	M[b]	N_T[b]	Temperature [K]	L[b]	d_l [Å] (k_l [kcal/mol·Å^2])[c]
REM1	16	16	200, 229, 262, 299, 342, 391, 448, 512, 586, 670, 766, 876, 1002, 1147, 1311, 1500	0	
REUS1, US1	14	1	300	14	0.0 (0.0)[d], 1.8 (1.2), 2.8 (1.2), 3.8 (1.2), 4.8 (1.2), 5.8 (1.2), 6.8 (1.2), 7.8 (1.2), 8.8 (1.2), 9.8 (1.2), 10.8 (1.2), 11.8 (1.2), 12.8 (1.2), 13.8 (1.2)
REUS2, US2	16	4	250, 315, 397, 500	4	0.0 (0.0), 7.8 (0.3), 10.8 (0.3), 13.8 (0.3)

[a]REM, REUS, and US stand for an original replica-exchange simulation, replica-exchange umbrella sampling simulation, and conventional umbrella sampling simulation, respectively.

[b]M, N_T, and L are the total numbers of replicas, temperatures, and restraining potentials, respectively [see Eqs. (16) and (24)]. In REUS2 and US2 we set $M=N_T\times L$ for simplicity. We remark that this relation is not always required. For instance, the 16 replicas could have 16 different temperatures with 16 different restraining potentials (i.e., $M=N_T=L=16$).

[c]d_l and k_l ($l=1,\ldots,L$) are the strengths and the midpoints of the restraining potentials, respectively [see Eq. (25)].

[d]The parameter value 0.0 (0.0) means that the restraining potential is null, i.e., $V_l=0$.

tions (REUS1 and REUS2), and two conventional umbrella sampling simulations (US1 and US2). The purpose of the present simulations is to test the effectiveness of the replica-exchange umbrella sampling with respect to the conventional umbrella sampling (REUS1 and REUS2 versus US1 and US2). The original replica-exchange simulation without umbrella potentials (REM1) was also made to set a reference standard for comparison. For REM1, replica exchange was tried every 20 time steps (or 10 fs), as in our previous work.[44] For REUS simulations, on the other hand, replica exchange was tried every 400 steps (or 200 fs), which is less frequent than in REM1. This is because we wanted to ensure sufficient time for system relaxation after λ-parameter exchange.

In REM1 there are 16 replicas with 16 different temperatures listed in Table I. The temperatures are distributed exponentially, following the optimal distribution found in Ref. 44. After every 10 fs of parallel MD simulations, eight pairs of replicas corresponding to neighboring temperatures were simultaneously exchanged, and the pairing was alternated between the two possible choices.[44]

For umbrella potentials, the O1 to H5 hydrogen-bonding distance, or ''end-to-end distance,'' was chosen as the reaction coordinate ξ and the harmonic restraining potentials of ξ in Eq. (25) were imposed. The force constants, $k_{\swarrow}$, and the midpoint positions, $d_{\swarrow}$, are listed in Table I.

In REUS1 and US1, 14 replicas were simulated with the same set of umbrella potentials at $T=300$ K. The first parameter value, 0.0 (0.0), in Table I means that the restraining potential is null, i.e., $V_{\swarrow}=0$. The remaining 13 sets of parameters are the same as those adopted in Ref. 51. Let us order the umbrella potentials, $V_{\swarrow}$ in Eq. (24), in the increasing order of the midpoint value $d_{\swarrow}$, i.e., the same order that appears in Table I. We prepared replicas so that the potential energy for each replica includes exactly one umbrella potential (here, we have $M=L=14$). Namely, in Eq. (24) for $\boldsymbol{\lambda}=\boldsymbol{\lambda}_m$ we set

$$\lambda_m^{(\swarrow)}=\delta_{\swarrow,m}, \tag{30}$$

where $\delta_{k,l}$ is Kronecker's delta function, and we have

$$E_{\boldsymbol{\lambda}_m}(q^{[i]})=E_0(q^{[i]})+V_m(q^{[i]}). \tag{31}$$

The difference between REUS1 and US1 is whether replica exchange is performed or not during the parallel MD simulations. In REUS1 seven pairs of replicas corresponding to ''neighboring'' umbrella potentials, V_m and V_{m+1}, were simultaneously exchanged after every 200 fs of parallel MD simulations, and the pairing was alternated between the two possible choices. (Other pairings will have much smaller acceptance ratios of replica exchange.) The acceptance criterion for replica exchange is given by Eq. (17), where Eq. (18) now reads (with the fixed inverse temperature $\beta=1/300k_B$)

$$\Delta=\beta(V_m(q^{[j]})-V_m(q^{[i]})-V_{m+1}(q^{[j]})+V_{m+1}(q^{[i]})), \tag{32}$$

where replica i and j, respectively, have umbrella potentials V_m and V_{m+1} before the exchange.

In REUS2 and US2, 16 replicas were simulated at four different temperatures with four different restraining potentials (there are $L=4$ umbrella potentials at $N_T=4$ temperatures, making the total number of replicas $M=N_T\times L=16$; see Table I). We can introduce the following labeling for the parameters characterizing the replicas:

$$\begin{aligned}&\boldsymbol{\Lambda}_m=(T_m,\boldsymbol{\lambda}_m) \quad \rightarrow \quad \boldsymbol{\Lambda}_{I,J}=(T_I,\boldsymbol{\lambda}_J),\\ &(m=1,\ldots,M) \quad (I=1,\ldots,N_T, J=1,\ldots,L).\end{aligned} \tag{33}$$

The potential energy is given by Eq. (31) with the replacement: $m\rightarrow J$. Let us again order the umbrella potentials, V_J, and the temperatures, T_I, in the same order that appear in Table I. The difference between REUS2 and US2 is whether replica exchange is performed or not during the MD simula-

TABLE II. Acceptance ratios of replica exchange in REM1.

Pair of temperatures	Acceptance ratio
200↔229	0.430
229↔262	0.433
262↔299	0.433
299↔342	0.428
342↔391	0.430
391↔448	0.423
448↔512	0.429
512↔586	0.427
586↔670	0.434
670↔766	0.437
766↔876	0.445
876↔1002	0.446
1002↔1147	0.446
1147↔1311	0.454
1311↔1500	0.452

TABLE III. Acceptance ratios of replica exchange in REUS1.

Pair of restraint parameters	Acceptance ratio
0.0 (0.0)↔1.8 (1.2)	0.202
1.8(1.2)↔2.8 (1.2)	0.210
2.8 (1.2)↔3.8 (1.2)	0.174
3.8 (1.2)↔4.8 (1.2)	0.161
4.8 (1.2)↔5.8 (1.2)	0.223
5.8 (1.2)↔6.8 (1.2)	0.155
6.8 (1.2)↔7.8 (1.2)	0.211
7.8 (1.2)↔8.8 (1.2)	0.229
8.8(1.2)↔9.8 (1.2)	0.119
9.8 (1.2)↔10.8 (1.2)	0.276
10.8 (1.2)↔11.8 (1.2)	0.156
11.8 (1.2)↔12.8 (1.2)	0.138
12.8 (1.2)↔13.8 (1.2)	0.383

tions. In REUS2 we performed the following replica-exchange processes alternately after every 200 fs of parallel MD simulations:

(1) Exchange pairs of replicas corresponding to neighboring temperatures, T_I and T_{I+1} (i.e., exchange replicas i and j that respectively correspond to parameters $\mathbf{\Lambda}_{I,J}$ and $\mathbf{\Lambda}_{I+1,J}$). (We refer to this process as T-exchange.)
(2) Exchange pairs of replicas corresponding to ''neighboring'' umbrella potentials, V_J and V_{J+1} (i.e., exchange replicas i and j that respectively correspond to parameters $\mathbf{\Lambda}_{I,J}$ and $\mathbf{\Lambda}_{I,J+1}$). (We refer to this process as λ-exchange.)

In each of the above processes, two pairs of replicas were simultaneously exchanged, and the pairing was further alternated between the two possibilities. The acceptance criterion for these replica exchanges is given by Eq. (17), where Eq. (18) now reads

$$\Delta=(\beta_I-\beta_{I+1})(E_0(q^{[j]})+V_J(q^{[j]})-E_0(q^{[i]}) -V_J(q^{[i]})), \tag{34}$$

for T-exchange, and

$$\Delta=\beta_I(V_J(q^{[j]})-V_J(q^{[i]})-V_{J+1}(q^{[j]})+V_{J+1}(q^{[i]})), \tag{35}$$

for λ-exchange. By this procedure, the random walk in the reaction coordinate space as well as in temperature space can be realized. Note that we carry out the velocity rescaling of Eq. (8) in T-exchange. In principle, we can also introduce a similar velocity rescaling in λ-exchange to the two relevant atoms O1 and H5 in order to adjust for the exchange of the restraining potentials (because the restraining force acts only on O1 and H5). We also incorporated this rescaling but did not see much improvement in performance. The results presented below are thus those from no velocity rescaling in λ-exchange.

We now give the details of the results obtained in the present work. First of all, we examine whether the replica-exchange processes properly occurred in REM and REUS simulations. One criterion for the optimal performance is: whether the acceptance ratio of replica exchange is uniform and sufficiently large or not. In Tables II–IV we list the acceptance ratios of replica exchange corresponding to the adjacent pairs of temperatures or the restraining potentials. In all cases the acceptance ratios are almost uniform and large enough (>10 %); all simulations indeed performed properly. In particular, the acceptance ratios for exchanging adjacent temperatures are significantly uniform in all cases, implying that the exponential temperature distributions of Ref. 44 are again optimal. However, the acceptance ratios for exchanging adjacent restraining potentials are not perfectly uniform, and there is some room for fine tuning. The acceptance ratio for exchanging restraining potentials depends on the strength of the force constants, k_l, [see Eq. (25)] and we weakened the value from 1.2 kcal/mol·Å^2 in REUS1 to 0.3 kcal/mol·Å^2 in REUS2 in order to have sufficient replica exchanges in REUS2. This is because we have a much smaller number

TABLE IV. Acceptance ratios of replica exchange in REUS2.

Temperature	Pair of restraint parameters	Acceptance ratio
250	0.0 (0.0)↔7.8 (0.3)	0.149
250	7.8 (0.3)↔10.8 (0.3)	0.104
250	10.8 (0.3)↔13.8 (0.3)	0.127
315	0.0 (0.0)↔7.8 (0.3)	0.250
315	7.8 (0.3)↔10.8 (0.3)	0.105
315	10.8 (0.3)↔13.8 (0.3)	0.120
397	0.0 (0.0)↔7.8 (0.3)	0.363
397	7.8 (0.3)↔10.8 (0.3)	0.135
397	10.8 (0.3)↔13.8 (0.3)	0.160
500	0.0 (0.0)↔7.8 (0.3)	0.483
500	7.8 (0.3)↔10.8 (0.3)	0.185
500	10.8 (0.3)↔13.8 (0.3)	0.228
Restraint parameters	**Pair of temperatures**	**Acceptance ratio**
0.0 (0.0)	250↔315	0.193
0.0 (0.0)	315↔397	0.186
0.0 (0.0)	397↔500	0.189
7.8 (0.3)	250↔315	0.174
7.8 (0.3)	315↔397	0.179
7.8 (0.3)	397↔500	0.190
10.8 (0.3)	250↔315	0.189
10.8 (0.3)	315↔397	0.184
10.8 (0.3)	397↔500	0.195
13.8 (0.3)	250↔315	0.185
13.8 (0.3)	315↔397	0.184
13.8 (0.3)	397↔500	0.205

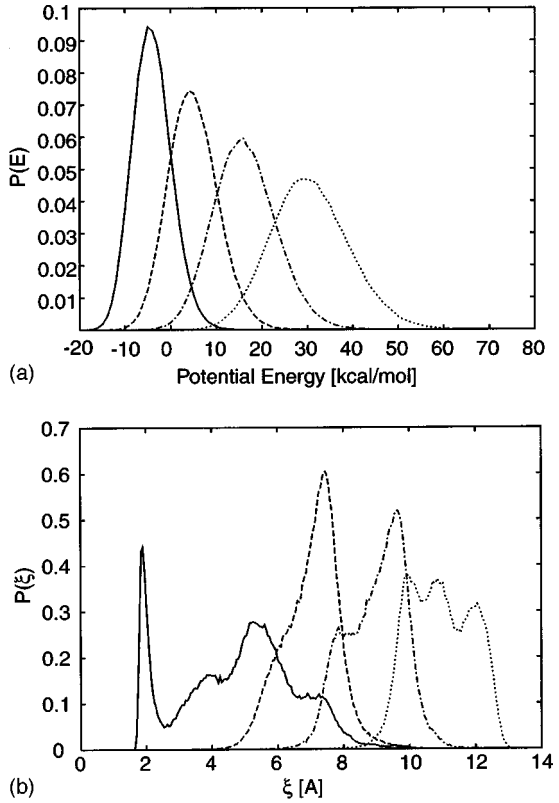

FIG. 1. Probability distributions obtained from the replica-exchange umbrella sampling simulation (REUS2). (a) The canonical probability distributions of the unbiased potential energy E_0 at the four chosen temperatures (the curves from left to right correspond to $T=$ 250, 315, 397, 500 K). The results are for the parameters $\mathbf{\Lambda}_{I,1}$ ($I=1,\ldots,4$), i.e., for the case of no restraining potentials (see Table I). (b) The probability distributions of the reaction coordinate ξ, the distance between the atoms O1 and H5, with the four chosen restraining potentials [the curves from left to right correspond to $d_{\angle}$ [Å] ($k_{\angle}$ [kcal/mol·Å^2])$=$ 0.0 (0.0), 7.8 (0.3), 10.8 (0.3), 13.8 (0.3)]. The results are for the parameters $\mathbf{\Lambda}_{2,J}$ ($J=1,\ldots,4$), i.e., for the temperature $T=315$ K (see Table I).

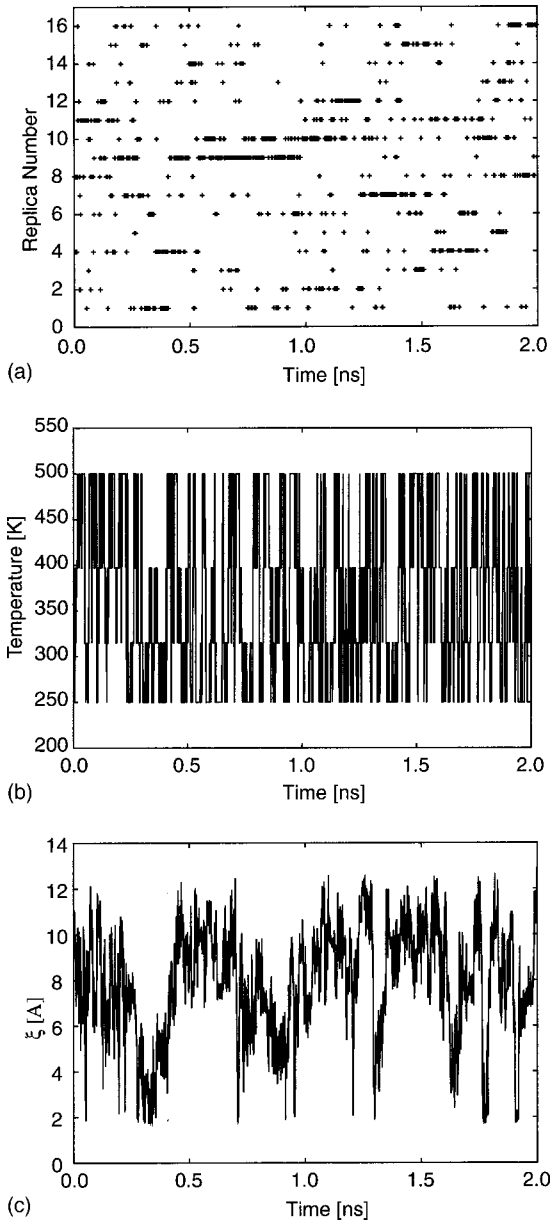

FIG. 2. Time series of the replica-exchange umbrella sampling simulation (REUS2). (a) Replica exchange for the parameter $\mathbf{\Lambda}_{1,1}=(T_1,\boldsymbol{\lambda}_1)$ (i.e., $T_1=250$ K and $k_1=d_1=0.0$, see Table I). (b) Temperature exchange for one of the replicas (replica 1). (c) The reaction coordinate ξ for one of the replicas (replica 1).

of restraining potentials in REUS2 than in REUS1 (3 versus 13), and yet both simulations have to cover the same range of reaction coordinate ξ, i.e., from 0 Å to 13.8 Å .

In order to have sufficient replica exchanges between neighboring temperatures and between neighboring restraining potentials, the probability distributions corresponding to neighboring parameters should have enough overlaps. In Fig. 1(a) the canonical probability distributions of the unbiased potential energy E_0 at the four chosen temperatures are shown. The results are for the parameters $\mathbf{\Lambda}_{I,1}$ ($I=1,\ldots,4$), i.e., for the case of no restraining potentials, and were obtained from the REUS2 simulation. In Fig. 1(b) the probability distributions of the reaction coordinate ξ with the four chosen restraining potentials are shown. The results are for the parameters $\mathbf{\Lambda}_{2,J}$ ($J=1,\ldots,4$), i.e., for the temperature $T=315$ K, and were also obtained from the REUS2 simulation. In both figures we do observe sufficient overlaps in pairs of the distributions corresponding to the neighboring parameter values, and this is reflected in the reasonable acceptance ratios listed in Table IV.

In order to further confirm that our REM simulations performed properly, we have to examine the time series of various quantities and observe random walks. For instance, in Fig. 2 the trajectories of a few quantities in REUS2 are shown. In Fig. 2(a) we show the time series of replica exchange for the parameter $\mathbf{\Lambda}_{1,1}=(T_1,\boldsymbol{\lambda}_1)$ (i.e., $T_1=250$ K and $k_1=d_1=0.0$). We do observe a random walk in replica space, and we see that all the replicas frequently visited the parameter value $\mathbf{\Lambda}_{1,1}$.

The complementary picture to this is the time series of T-exchange and λ-exchange for each replica. Free random walks both in ''temperature space'' and in ''restraining potential space'' were indeed observed. For instance, the time series of temperature exchange for one of the replicas (replica 1) is shown in Fig. 2(b). The corresponding time series of the reaction coordinate ξ, the distance between atoms O1 and H5, for the same replica is shown in Fig. 2(c). We see

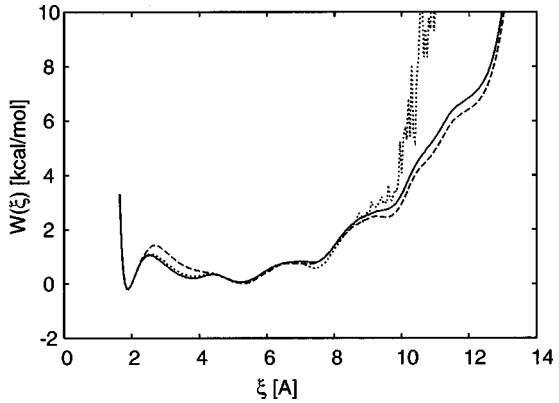

FIG. 3. The PMF along the reaction coordinate ξ at $T=300$ K. The dotted, solid, and dashed curves were obtained from the original REM (REM1), the replica-exchange umbrella sampling (REUS1), and the conventional umbrella sampling (US1), respectively.

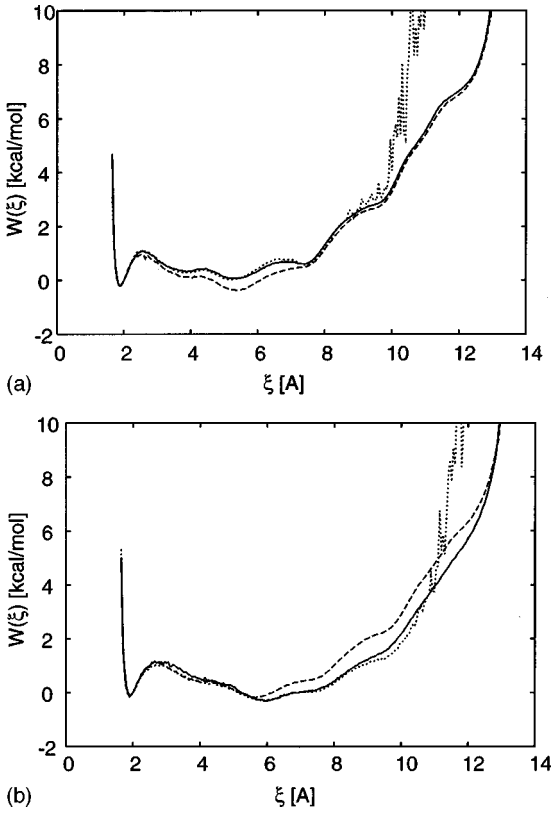

FIG. 4. The PMF along the reaction coordinate ξ at two temperatures. (a) The PMF at $T=300$ K. The dotted, solid, and dashed curves were obtained from the original REM (REM1), the replica-exchange umbrella sampling (REUS2), and the conventional umbrella sampling (US2), respectively. (b) The PMF at $T=500$ K. The dotted, solid, and dashed curves were obtained from the original REM (REM1), the replica-exchange umbrella sampling (REUS2), and the conventional umbrella sampling (US2), respectively.

that the conformational sampling along the reaction coordinate is significantly enhanced. In the blocked alanine trimer, the reaction coordinate ξ can be classified into three regions:[51] the helical region ($\xi<3$ Å), the turn region (3 Å $<\xi<$ 7 Å), and the extended region ($\xi>$ 7 Å). Thus, Fig. 2(c) implies that helix-coil transitions frequently occurred during the replica-exchange simulation, whereas in the conventional canonical simulations such a frequent folding and unfolding process cannot be seen.

After confirming that the present REM and REUS simulations performed properly, we now present and compare the physical quantities calculated by these simulations. In Fig. 3 the potentials of mean force (PMF) of the unbiased system along the reaction coordinate ξ at $T=300$ K are shown. The results are from REM1, REUS1, and US1 simulations. For these calculations, the WHAM equations of Eqs. (26) and (27) were solved by iteration first, and then Eq. (29) was used to obtain the PMF. We remark that for biomolecular systems the results obtained from the WHAM equations are insensitive to the values of g_m in Eq. (26).[4] Hence, we set $g_m=$ constant in the present article. From Fig. 3 we see that the PMF curves obtained by REM1 and REUS1 are essentially identical for low values of ξ ($\xi<7$ Å). The two PMF curves start deviating slightly, as ξ gets larger, and for $\xi>9$ Å the agreement completely deteriorates. The disagreement comes from the facts that the average ξ at the highest temperature in REM1 ($T_{16}=1500$ K) is $<\xi>_{T_{16}}=8.0$ Å and that the original REM with *T*-exchange only cannot sample accurately the region where ξ is much larger than $<\xi>_{T_{16}}$. These two simulations were performed under very different conditions: One was run at different temperatures without restraining potentials and the other at one temperature with many restraining potentials (see Table I). We thus consider the results to be quite reliable for ($\xi<9$ Å).

On the other hand, the PMF obtained by US1 is relatively larger than those obtained by REM1 and REUS1 in the region of 2 Å $<\xi<$ 4 Å, which corresponds to the structural transition state between the α-helical and turn structures. This suggests that US1 got trapped in states of energy local minima at $T=300$ K. In the region of completely extended structures ($\xi>9$ Å), the results of REUS1 and US1 are similar but the discrepancy is again non-negligible. We remark that at $T=300$ K the PMF is the lowest for $\xi=2$ Å, which implies that the α-helical structure is favored at this temperature.

We next study the temperature dependence of physical quantities obtained from the REM1, REUS2, and US2 simulations. In Fig. 4(a) we show the PMF again at $T=300$ K. We observe that the PMF curves from REM1 and REUS2 are essentially identical for $\xi<9$ Å and that they deviate for $\xi>9$ Å, because the results for REM1 are not reliable in this region, as noted above. In fact, by comparing Figs. 3 and 4(a), we find that the PMF obtained from REUS1 and REUS2 are almost in complete agreement at $T=300$ K in the entire range of ξ values shown. On the other hand, we observe a discrepancy between REUS2 and US2 results. The PMF curve for US2 is significantly less than that for REUS2 in the region 2 Å $<\xi<$ 8 Å. Note that the PMF curves for US1 and US2 are completely in disagreement [compare Figs. 3 and 4(a)].

In Fig. 4(b) we show the PMF at $T=500$ K, which we obtained from REM1, REUS2, and US2 simulations. We again observe that the results from REM1 and REUS2 are in good agreement for a wide range of ξ values. We find that the results from REM1 do not significantly deteriorate until $\xi>11$ Å at $T=500$ K, whereas it did start deviating badly for

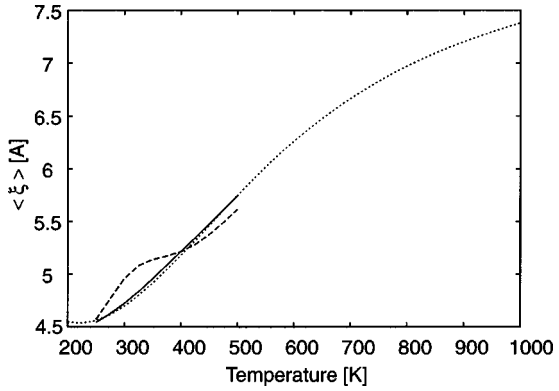

FIG. 5. Average values of the reaction coordinate ξ as a function of temperature. The dotted, solid, and dashed curves were obtained from the original REM (REM1), the replica-exchange umbrella sampling (REUS2), and the conventional umbrella sampling (US2), respectively. Although the highest temperature in REM1 is 1500 K, only the results for the temperature range between 200 and 1000 K are shown for REM1. Since the lowest and highest temperatures in REUS2 and US2 are, respectively, 250 and 500 K, only the results between these temperatures are shown for these simulations.

$\xi > 9$ Å at $T = 300$ K. The PMF curve for US2 deviates strongly from the REUS2 results for $\xi > 6$ Å and is much larger than that of REUS2 (and REM1) in this region. We remark that at $T = 500$ K the PMF is the lowest for $\xi \approx 6$ Å, which implies that extended structures are favored at this temperature.

In Fig. 5 we show the average values of the reaction coordinate ξ as a function of temperature. The results are again from the REM1, REUS2, and US2 simulations. The expectation values were calculated from Eq. (28). We find that the average reaction coordinate, or the average end-to-end distance, grows as the temperature is raised, reflecting the unfolding of the peptide upon increased thermal fluctuations. Again we observe an agreement between REM1 and REUS2, whereas the results of US2 deviate.

Let us emphasize that the total length of the MD simulations was the same (2 ns) for each replica in all the simulations performed. Hence, we have shown that the replica-exchange umbrella sampling can give much more accurate free-energy profiles along a reaction coordinate than the conventional umbrella sampling.

IV. CONCLUSIONS

In this article we have presented a multidimensional extension of the original replica-exchange method. One example of this approach is the combination of the replica-exchange method with the umbrella sampling, which we refer to as the *replica-exchange umbrella sampling* (REUS). While pairs of replicas with different temperatures are exchanged during the simulation in the original replica-exchange method, pairs of replicas with different temperatures and/or different biasing potentials for the umbrella sampling are exchanged in REUS. This greatly enhances the sampling of the conformational space and allows accurate calculations of free energy in a wide temperature range from a single simulation run, using the weighted histogram analysis method. The difference between REUS and the conventional umbrella sampling is just whether the replica-exchange process is performed or not. Only minor modifications to the conventional umbrella sampling method are necessary. However, the advantage of REUS over the umbrella sampling is significant, and the effectiveness was established with the system of an alanine trimer.

ACKNOWLEDGMENTS

Our simulations were performed on the Hitachi and other computers at the Research Center for Computational Science, Okazaki National Research Institutes. A part of the computation was done also at the Center for Promotion of Computational Science and Engineering of Japan Atomic Energy Research Institute and Computer Center of the National Institute of Genetics. This work is supported, in part, by a grant from the Research for the Future Program of the Japan Society for the Promotion of Science (Grant No. JSPS-RFTF98P01101).

[1] U. H. E. Hansmann and Y. Okamoto, in *Annual Reviews of Computational Physics VI*, edited by D. Stauffer (World Scientific, Singapore, 1999), p. 129.
[2] A. M. Ferrenberg and R. H. Swendsen, Phys. Rev. Lett. **61**, 2635 (1988).
[3] A. M. Ferrenberg and R. H. Swendsen, Phys. Rev. Lett. **63**, 1195 (1989).
[4] S. Kumar, D. Bouzida, R. H. Swendsen, P. A. Kollman, and J. M. Rosenberg, J. Comput. Chem. **13**, 1011 (1992).
[5] B. A. Berg and T. Neuhaus, Phys. Lett. B **267**, 249 (1991); Phys. Rev. Lett. **68**, 9 (1992).
[6] A. P. Lyubartsev, A. A. Martinovski, S. V. Shevkunov, and P. N. Vorontsov-Velyaminov, J. Chem. Phys. **96**, 1776 (1992).
[7] E. Marinari and G. Parisi, Europhys. Lett. **19**, 451 (1992).
[8] K. Hukushima and K. Nemoto, J. Phys. Soc. Jpn. **65**, 1604 (1996); K. Hukushima, H. Takayama, and K. Nemoto, Int. J. Mod. Phys. C **7**, 337 (1996).
[9] R. H. Swendsen and J.-S. Wang, Phys. Rev. Lett. **57**, 2607 (1986).
[10] C. J. Geyer, in *Computing Science and Statistics, Proceedings 23rd Symp. on the Interface*, edited by E. M. Keramidas (Interface Foundation, Fairfax Station, 1991), p. 156.
[11] M. C. Tesi, E. J. J. van Rensburg, E. Orlandini, and S. G. Whittington, J. Stat. Phys. **82**, 155 (1996).
[12] E. Marinari, G. Parisi, and J. J. Ruiz-Lorenzo, in *Spin Glasses and Random Fields*, edited by A. P. Young (World Scientific, Singapore, 1998), p. 59.
[13] U. H. E. Hansmann and Y. Okamoto, J. Comput. Chem. **14**, 1333 (1993).
[14] U. H. E. Hansmann and Y. Okamoto, Physica A **212**, 415 (1994).
[15] M. H. Hao and H. A. Scheraga, J. Phys. Chem. **98**, 4940 (1994).
[16] Y. Okamoto and U. H. E. Hansmann, J. Phys. Chem. **99**, 11276 (1995).
[17] A. Kidera, Proc. Natl. Acad. Sci. U.S.A. **92**, 9886 (1995).
[18] A. Kolinski, W. Galazka, and J. Skolnick, Proteins **26**, 271 (1996).
[19] N. Urakami and M. Takasu, J. Phys. Soc. Jpn. **65**, 2694 (1996).
[20] S. Kumar, P. Payne, and M. Vśquez, J. Comput. Chem. **17**, 1269 (1996).
[21] U. H. E. Hansmann, Y. Okamoto, and F. Eisenmenger, Chem. Phys. Lett. **259**, 321 (1996).
[22] N. Nakajima, H. Nakamura, and A. Kidera, J. Phys. Chem. **101**, 817 (1997).
[23] H. Noguchi and K. Yoshikawa, Chem. Phys. Lett. **278**, 184 (1997).
[24] U. H. E. Hansmann and F. Eisenmenger, J. Phys. Chem. B **101**, 3304 (1997).
[25] J. Higo, N. Nakajima, H. Shirai, A. Kidera, and H. Nakamura, J. Comput. Chem. **18**, 2086 (1997).
[26] A. Kolinski, W. Galazka, and J. Skolnick, J. Chem. Phys. **108**, 2608 (1998).
[27] C. Bartels and M. Karplus, J. Phys. Chem. B **102**, 865 (1998).
[28] Y. Iba, G. Chikenji, and M. Kikuchi, J. Phys. Soc. Jpn. **67**, 3327 (1998).
[29] N. Nakajima, Chem. Phys. Lett. **288**, 319 (1998).
[30] M. H. Hao and H. A. Scheraga, J. Mol. Biol. **277**, 973 (1998).
[31] H. Shirai, N. Nakajima, J. Higo, A. Kidera, and H. Nakamura, J. Mol. Biol. **278**, 481 (1998).
[32] M. Schaefer, C. Bartels, and M. Karplus, J. Mol. Biol. **284**, 835 (1998).
[33] C. Bartels, R. H. Stote, and M. Karplus, J. Mol. Biol. **284**, 1641 (1998).

[34] U. H. E. Hansmann and Y. Okamoto, J. Phys. Chem. B **103**, 1595 (1999).
[35] S. Ono, N. Nakajima, J. Higo, and H. Nakamura, Chem. Phys. Lett. **312**, 247 (1999).
[36] A. Mitsutake and Y. Okamoto, J. Chem. Phys. **112**, 10638 (2000).
[37] A. Irbäck and F. Potthast, J. Chem. Phys. **103**, 10298 (1995).
[38] U. H. E. Hansmann and Y. Okamoto, Phys. Rev. E **54**, 5863 (1996).
[39] A. Irbäck, C. Peterson, F. Potthast, and O. Sommelius, J. Chem. Phys. **107**, 273 (1997).
[40] U. H. E. Hansmann and Y. Okamoto, J. Comput. Chem. **18**, 920 (1997).
[41] U. H. E. Hansmann, Chem. Phys. Lett. **281**, 140 (1997).
[42] M. Falcioni and M. W. Deem, J. Chem. Phys. **110**, 1754 (1999).
[43] A. Irbäck and E. Sandelin, J. Chem. Phys. **110**, 12256 (1999).
[44] Y. Sugita and Y. Okamoto, Chem. Phys. Lett. **314**, 141 (1999).
[45] R. Yamamoto and W. Kob, Phys. Rev. E **61**, 5473 (2000).
[46] K. Hukushima, Phys. Rev. E **60**, 3606 (1999).
[47] Q. Yan and J. J. de Pablo, J. Chem. Phys. **111**, 9509 (1999).
[48] G. M. Torrie and J. P. Valleau, J. Comput. Phys. **23**, 187 (1977).
[49] S. H. Northrup, M. R. Pear, C.-Y. Lee, J. A. McCammon, and M. Karplus, Proc. Natl. Acad. Sci. USA **79**, 4035 (1982).
[50] W. L. Jorgensen, J. Phys. Chem. **87**, 5304 (1983).
[51] E. M. Boczko and C. L. Brooks III, J. Phys. Chem. **97**, 4509 (1993).
[52] S. Yun-yu, A. E. Mark, W. Cun-xin, H. Fuhua, H. J. C. Berendsen, and W. F. van Gunsteren, Protein Eng. **6**, 289 (1993).
[53] S. Kumar, J. M. Rosenberg, D. Bouzida, R.H. Swendsen, and P. A. Kollman, J. Comput. Chem. **16**, 1339 (1995).
[54] M. Saito and R. Tanimura, Chem. Phys. Lett. **236**, 156 (1995).
[55] E. M. Boczko and C. L. Brooks III, Science **269**, 393 (1995).
[56] Y. Sugita and A. Kitao, Proteins **30**, 388 (1998).
[57] Y. Sugita and A. Kitao, Biophys. J. **75**, 2178 (1998).
[58] X. Kong and C. L. Brooks III, J. Chem. Phys. **105**, 2414 (1996).
[59] Z. Guo, C. L. Brooks III, and X. Kong, J. Phys. Chem. Soc. B **102**, 2032 (1998).
[60] M. Ikeguchi, S. Shimizu, K. Tazaki, S. Nakamura, and K. Shimizu, Chem. Phys. Lett. **288**, 333 (1998).
[61] N. Metropolis, A. W. Rosenbluth, M. N. Rosenbluth, A. H. Teller, and E. Teller, J. Chem. Phys. **21**, 1087 (1953).
[62] S. J. Weiner, P. A. Kollman, D. T. Nguyen, and D. A. Case, J. Comput. Chem. **7**, 230 (1986).
[63] A. Kitao, S. Hayward, and N. Gō, Proteins **33**, 496 (1998).
[64] K. Morikami, T. Nakai, A. Kidera, M. Saito, and H. Nakamura, Comput. Chem. **16**, 243 (1992).
[65] W. G. Hoover, A. J. C. Ladd, and B. Moran, Phys. Rev. Lett. **48**, 1818 (1982).
[66] D. J. Evans and G. P. Morris, Phys. Lett. A **98**, 433 (1983).